β^- decay of exotic P and S isotopes with neutron number near 28

Vandana Tripathi,[1,*] Soumik Bhattacharya,[1] E. Rubino,[1] C. Benetti,[1] J. F. Perello,[1] S. L. Tabor,[1] S. N. Liddick,[2,3,4] P. C. Bender,[5] M. P. Carpenter,[6] J. J. Carroll,[7] A. Chester,[2,3] C. J. Chiara,[7] K. Childers,[2,4] B. R. Clark,[8] B. P. Crider,[8] J. T. Harke,[9] B. Longfellow,[2,10] R. S. Lubna,[3] S. Luitel,[8] T. H. Ogunbeku,[8] A. L. Richard,[2,9] S. Saha,[5] N. Shimizu,[11] O. A. Shehu,[8] Y. Utsuno,[12,13] R. Unz,[8] Y. Xiao,[8] S. Yoshida,[14] and Yiyi Zhu[5]

[1]*Department of Physics, Florida State University, Tallahassee, Florida 32306, USA*
[2]*National Superconducting Cyclotron Laboratory, Michigan State University, East Lansing, Michigan 48824, USA*
[3]*Facility for Rare Isotope Beams, Michigan State University, East Lansing, Michigan 48824, USA*
[4]*Department of Chemistry, Michigan State University, East Lansing, Michigan 48824, USA*
[5]*Department of Physics, University of Massachusetts Lowell, Lowell, Massachusetts 01854, USA*
[6]*Argonne National Laboratory, Argonne, Illinois 60439, USA*
[7]*DEVCOM/Army Research Laboratory, Adelphi, Maryland 20783 USA*
[8]*Department of Physics and Astronomy, Mississippi State University, Mississippi State, Mississippi 39762, USA*
[9]*Lawrence Livermore National Laboratory, Livermore, California 94550, USA*
[10]*Department of Physics and Astronomy, Michigan State University, East Lansing, Michigan 48824, USA*
[11]*Center for Computational Sciences, University of Tsukuba, Tennodai, Tsukuba 305-8577, Japan*
[12]*Advanced Science Research Center, Japan Atomic Energy Agency, Tokai, Ibaraki 319-1195, Japan*
[13]*Center for Nuclear Study, University of Tokyo, Hongo, Bunkyo-ku, Tokyo 113-0033, Japan*
[14]*Liberal and General Education Center, Institute for Promotion of Higher Academic Education, Utsunomiya University, Mine, Utsunomiya, Tochigi 321-8505, Japan*

(Received 24 September 2022; accepted 28 November 2022; published 13 December 2022)

β^- decay of very neutron-rich isotopes of P and S, studied at the National Superconducting Cyclotron Laboratory using the Beta Counting Station consisting of a Double Sided Strip Detector surrounded by clovers detectors for observing delayed γ transitions, is reported here. β-decay half-lives and delayed neutron emission probabilities were extracted for ^{42,43,44}P and ^{44,46}S by analyzing spatial and temporal correlations between implants and decay events in the Si detector with further coincidence with γ transitions. Detection of delayed γ rays allowed for the identification of negative-parity 1p1h states in ^{42}S for the first time, also constraining the parent (^{42}P) spin/parity to 2^- or 3^-. For the most exotic isotope studied, ^{46}S, no strong γ transition was observed unlike lighter even-even S isotopes, thus implying the shift of Gamow-Teller strength distribution to higher energies. Comparison of experimental observations to detailed shell-model calculations using the SDPFSDG-MU interaction allowed us to infer the importance and role of first forbidden β transitions as the neutron number approaches and then exceeds $N = 28$.

DOI: 10.1103/PhysRevC.106.064314

I. INTRODUCTION

The $N = 28$ neutron magic number is one that originates from the large spin-orbit splitting of the $0f$ orbital, with the $f_{7/2}$ getting separated and forming its own shell above the $N = 20$ shell gap and the $f_{5/2}$ joining the $1p$ orbitals to form the fp shell. Focusing on the $N = 28$ nuclei isotones: For ^{48}Ca the N = 28 gap is large, demonstrated by the near-spherical nature of the ^{48}Ca ground state and its high-lying excited states. However, as protons are removed from the *sd* shell, the aforementioned shell gap gets diluted. Just two protons fewer, for ^{46}Ar the energy of the first excited 2^+ state falls sharply [1], while another two protons lower, ^{44}S is a deformed nucleus [2,3] with coexisting spherical and prolate ground shapes [4,5]. Even ^{43}S with $N = 27$ shows a signature of the disappearing $N = 28$ gap with the inversion of the $0f_{7/2}$ and $1p_{3/2}$ orbitals [6]. Below ^{44}S in the isotonic chain, both ^{42}Si and ^{40}Mg are considered deformed with an oblate shape for Si and prolate shape for Mg [7].

Along with the degeneracy of the $\nu(fp)$ orbitals with the filling of the $0f_{7/2}$ orbital is the reduction of the spacing of the proton $1s_{1/2}$ and $0d_{3/2}$ orbitals [8]. For ^{37}P ($Z = 15; N = 22$), the first excited $3/2^+$ state is at 865 keV with a ground state of $1/2^+$; however, as the neutron number increases the $3/2^+$ falls down to 184 keV for ^{43}P at $N = 28$. These two effects together are responsible for the deformation in this region. For the Mg isotopes the deformation trend continues down to ^{32}Mg ($N = 20$). Thus, the roughly triangular region formed by ^{32,40}Mg and ^{46}Ar displays sudden changes in shape [9]. These structural changes affect the β-decay properties of these nuclei. The Gamow-Teller (GT) strength distribution depends on the deformation and affects the half-life ($T_{1/2}$) and β-delayed neutron emission probability (P_n).

*Corresponding author: vtripath@fsu.edu

The β decay of neutron-rich nuclei approaching the $N = 28$ magic number and beyond is not very well studied. These isotopes are also important for astrophysical and reaction network calculations and thus to understand the effect of evolving nuclear structure in this region on the β-decay properties is vital. One open question is to better understand the β-decay mechanism with neutrons and protons occupying orbitals in different shells leading to parent and daughter nuclei having opposite parities. The allowed GT transitions can populate high-lying states as has been observed in some heavier Zn and Ga isotopes near ^{78}Ni [10]; however, in our recent study of the β decay of ^{38,40}Si [11], clear indication of low-lying core excited states was seen which were well reproduced by large-scale shell-model calculations [12,13]. More information is needed to fully understand this issue. Another question relates to the large feeding to low-lying opposite-parity states found experimentally in many cases, which cannot be attributed to allowed GT transitions. Two possibilities exist, one is that first forbidden (FF) transitions are feeding these opposite-parity levels, while the other relates to γ decay (mainly $E1$ transitions) from GT-fed neutron-unbound resonance states to the low-lying states which can go largely undetected [14]. If the FF decays are important, then their effect should also be pronounced on the half-lives ($T_{1/2}$) and β-delayed neutron emission probabilities (P_n).

Recent large-scale shell-model calculations by Yoshida *et al.* [13,15], using the SDPFSDG-MU, have highlighted the significant influence of FF transitions on the half-life values and β-delayed neutron emission probabilities especially for isotopes with $N \approx 28$. In FF β decay, the electron-neutrino pair carries one unit of angular momentum and hence the decay involves a parity change with $\Delta J \leqslant 2$. As neutrons start filling up the $1p_{3/2}$ orbital, its transformation to a proton in the $0d_{3/2}$ orbital becomes feasible and thus FF transitions can compete with the allowed GT decay. Yoshida has documented the states that would be populated via FF transitions along with their $\log ft$ values for isotopes with $13 < Z < 20$ and $38 < N < 48$ based on shell-model (SM) calculations [15]. Prior to that, Warburton *et al.* [16] calculated FF transitions for less-exotic isotopes with $A \approx 40$, and as an example they predict a 1% branch to the 2_1^+ state at ≈3.2 MeV for the β decay of ^{36}P to ^{36}S. Another recent theoretical work, Marketin *et al.* [17], also highlighted that in certain regions of the nuclear chart (one being neutron-rich *sd*-shell nuclei), first-forbidden transitions constitute a large fraction of the total decay rate and must be taken into account consistently in modern evaluation of half-lives.

In the current work we studied the β^- decay of P and S isotopes around and beyond $N = 28$, namely ^{42,43,44}P and ^{44,46}S, to explore the aspects of β decay relevant for large neutron excess. For all these isotopes β-decay half-lives have been reported earlier [18], however, some with limited precision. Similarly, P_n values have been reported in an earlier work, both experiments performed at GANIL in its early implementation [19,20]. The current work, to our knowledge, will be the second reported measurement of half-lives and P_n values in this very exotic region of the chart of nuclides [21] and is the first to measure β-delayed γ rays to study excited states in the daughter nuclei (both β and βn). Negative-parity intruder states were observed here for the first time in ^{42}S following β^- decay of ^{42}P. The observation of γ transitions allowed us, in some cases, to confirm half-lives by following the characteristic γ rays in the daughter nucleus. We also used the intensity of γ transitions in the granddaughter nuclei in the β and βn chains to infer the β-delayed neutron emission probabilities. We confirm previous measurements of a 100% P_n for ^{43}P [20] following the γ transitions in ^{43}S and ^{43}Cl. Additionally, high P_n values have been derived for the $N > 28$ ^{44}P and ^{46}S. The experimental results are interpreted within configuration interaction shell-model calculations using the SDPFSDG-MU interaction [12,13].

II. EXPERIMENTAL SETUP

The experiment to investigate the β^- decay of very exotic $^{42-44}$P and ^{44,46}Si was carried out at the National Superconducting Cyclotron Laboratory (NSCL) [22] at Michigan State University. A ^{48}Ca primary beam, which is the best candidate to produce these fragments, was accelerated to 140 MeV/u and then fragmented on a thick Be target at the target position of the fragment separator, A1900 [23], to produce the nuclei of interest. A wedge-shaped Al degrader was positioned at the intermediate dispersive image of A1900 to increase the energy dispersion for different isotopes and hence provide a cleaner particle identification of the cocktail beam. Two magnetic rigidity settings of the A1900, with 1% and 2% momentum acceptance, were employed, with the larger momentum acceptance essential for the most exotic isotopes ^{44}P and ^{46}S.

The selected isotopes in the two settings were transported to the Beta Counting System (BCS) [24]. The heart of the BCS is a pixelated (40 strips × 40 strips) Double-Sided Silicon Strip Detector (DSSD). An Al degrader upstream ensured that the implants stopped at the middle of the ≈1 -mm-thick DSSD. The DSSD was followed by a Single-Sided Silicon Strip Detector (SSSD), which served as a veto detector. For the particular A1900 settings used for this experiment, a large flux of light particles was transmitted which needed to be eliminated to ensure good implant-β correlation. The DSSD recorded the time and position of implants (GeV energy depositions), as well as subsequent decays (keV-to-MeV energy depositions) by using dual gain preamplifiers. The implant rate was kept low, about 150/s on an average, to maximize the efficiency of correlating the implanted ion with the decay products. Two Si PIN detectors placed upstream of the DSSD provided the energy loss and time-of-flight information (along with the scintillator at the intermediate dispersive image of the A1900) for particle identification of the incoming implants. The DSSD and SSSD stack was surrounded by 16 Clover detectors to record the β-delayed γ rays with an efficiency of about 5% at 1 MeV. Efficiency was measured using a standard mixed γ-ray source, SRM-4275 from NIST, and ^{56}Co placed outside of the DSSD and then GEANT4 simulations were performed to correct for the dimensions of the DSSD. The SRM source provides photons from ^{125}Sb (with ^{125m}Te in equilibrium) and ^{154,155}Eu with energies ranging from 27 to 1596 keV while ^{56}Co allowed us to extend the energy range to 3.55 MeV. The data were collected event by event using the NSCL digital data acquisition system [25]. Each

channel provided its own time-stamp signal, which allowed coincidences and correlations to be built in the analysis. Along with the isotopes mentioned above, ^{43,45}S and ^{45,47}Cl were also transported to the BCS and they will be discussed in an upcoming publication.

III. EXPERIMENTAL RESULTS

A. P isotopes

As pointed out earlier, the half-lives and P_n values have been reported before for $^{42-44}$P [18–20] but no delayed γ emission was measured as the experimental setup did not include γ detection. For P with $Z = 15$, in the simple shell-model ordering of levels the odd proton would occupy the $1s_{1/2}$ orbital; however, with neutron number inching toward $N = 28$ the $\pi 1s_{1/2}$ and $\pi 0d_{3/2}$ orbitals are almost degenerate [8], leading to increased occupancy of the $\pi 0d_{3/2}$ orbital. For the odd-odd ^{42}P, theoretical predictions favor a 0^- ground state [26] with a proposed configuration of $\pi 0d^1_{3/2} \nu 1p^1_{3/2}$ and the same could be expected for ^{44}P though no experimental confirmation exists. Other spin states from the same configuration also lie close in energy in the calculations. In the nuclear physics picture where the decays of the nucleus are caused by transformation of the nucleon constituents, for the present case of β decay of P isotopes, one of the neutrons from either the fp or sd shells has to transform to a proton. As the $1s_{1/2}$ and $0d_{3/2}$ proton orbitals are not fully occupied, transformation of a $1s_{1/2}$ neutron to $1s_{1/2}$ proton or $0d_{5/2,3/2}$ neutron to $0d_{3/2}$ proton is possible (GT transitions), creating core neutron excited 1p1h states in the daughter. The change of $0f_{7/2}$ neutron is less likely as it will populate a state at higher excitation energy. Moreover, the $1p_{3/2}$ neutron can transform to a proton in $1p$ orbitals (GT decay) but can also switch to a $0d_{3/2}$ proton and that will create a 0p0h state of opposite parity in the daughter populated by a FF transition.

1. ^{42}P *($Z = 15$; $N = 27$)*

To extract the half-life of ^{42}P a decay curve was generated by histogramming the time difference between the position-correlated implanted ^{42}P ions and its decay products within a nine-pixel grid. The time correlation window was kept at 500 ms for this case. The fit to the decay curve as shown in Fig. 1(a) includes the contributions from the decay of daughter, ^{42}S, and β-delayed neutron daughter, ^{41}S, as well a background component to account for the long-lived activity not accounted for explicitly. Previously known half-lives of ^{41,42}S [27,28] and β-delayed neutron emission probability for ^{42}P (50(20)% [29]), were used for the fit shown. Changing the mean value of P_n by 20% did not affect the extracted half-life. As the statistics allowed, the obtained half-life of 47.1(20) ms was confirmed by fitting a decay curve which was gated on the β-delayed 903-keV transition from ^{42}S as shown in Fig. 1(b). This fit only included one exponential for the parent decay and a background due to the selectivity.

The β-delayed γ spectrum as recorded by the Clover array (addback between the four crystals was employed) is shown in Fig. 2 and the transitions associated with both ^{42}S and ^{41}S are marked. All the transitions except for the 3003(1)-keV

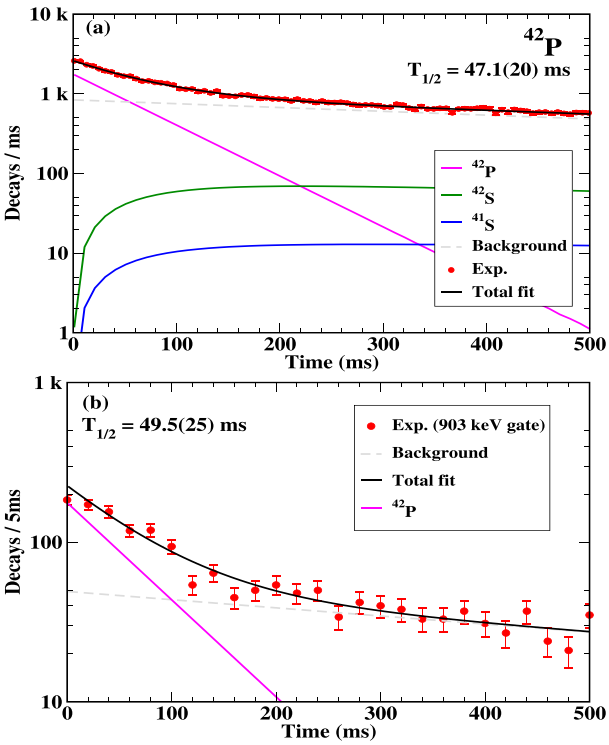

FIG. 1. (a) Decay curve derived for ^{42}P from β-correlated implants within a grid of nine pixels for 500 ms along with the fit used to extract half-life and the initial activity. The components of the fit are (i) exponential decay of parent, ^{42}P; (ii) exponential growth and decay of daughter nuclei, ^{42}S (β) and ^{41}S (βn); and (iii) exponential background. Known half-lives were used for the daughter nuclides [31]. (b) Decay curve gated by the 903-keV transition which represents the $2^+ \rightarrow 0^+$ transition in the daughter ^{42}S.

are found to be in coincidence with the 903(1)-keV line. The 3003-keV transition proceeds to the ground state directly and shows clear coincidence with the 2010(1)-keV γ ray. Some of the coincidence spectra are shown in Figs. 3(a)–3(c). The 903(1)-, 1820(1)-, 2100(1)-, 2679(2)-, and 3003(1)-keV transitions were known before from in-beam spectroscopy of ^{42}S [30] and the states generated are candidates for positive-parity states. The placement of the 2805-keV transition is tentative and differs from Ref. [30]. The 2010-keV and the high-energy γ transitions above 4 MeV [4110(2)-, 4243(2)-, 4591(1)-, and 4936(2)-keV] are associated with the β^- decay of ^{42}P and observed for the first time. The observed γ-ray are listed in Table I along with the absolute intensities per 100 decays.

The partial level scheme of ^{42}S based on the coincidences and energy and intensity balance is shown in Fig. 4. The absolute β branches were extracted using the measured efficiency of the Clover array and the total implanted ^{42}P nuclei (from the fit to the decay curve). Further, the logft values were extracted using the measured half-life ($T_{1/2}$) and the known Q_{β^-} value [31]. The levels above 5 MeV have logft values in the range for allowed GT transitions while the lower energy states could be populated via FF transitions as will be discussed later. The level schemes for the $\beta 1n$ daughter ^{41}S

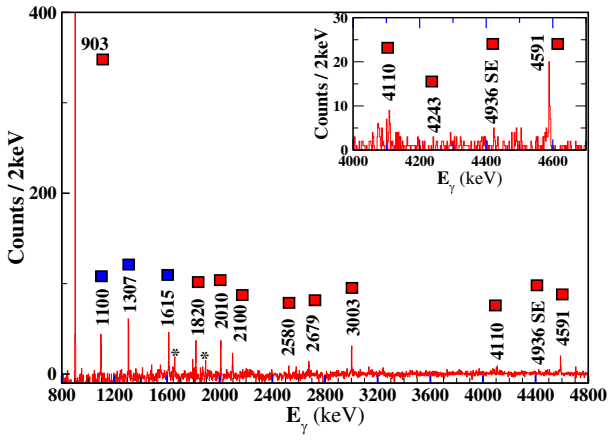

FIG. 2. Part of the β-delayed γ spectrum (background subtracted) up to 100 ms after a ^{42}P implant. The transitions marked with red squares belong to the $\beta 0n$ daughter ^{42}S with the 903-keV peak being the $2^+ \rightarrow 0^+$ transition in ^{42}S. The transitions from the $\beta 1n$ daughter ^{41}S are indicated by blue squares. The 1661- and 1895-keV transitions (*), though significant, could not be unambiguously assigned.

and the granddaughter ^{41}Cl were also confirmed and improved from literature information [30,32] and are shown in Fig. 5.

The β-delayed one-neutron emission probability was calculated by the counting of γ rays emitted by descendants in both the $\beta 0n$-decay and the $\beta 1n$-decay chains [33]. The absolute intensity of the 118-keV transition in ^{42}Cl (0.87% branching [34]) and the 130-keV transition in ^{41}Cl were used to evaluate a P_{1n} value of 39(6)%. The γ counts were corrected for the growth and decay of activities and the error quoted includes the uncertainty in the absolute branching of the 130-keV transition. This represents the lower limit of the P_n value and is consistent with the value of 50(20)% obtained in Ref. [29].

TABLE I. γ-ray energies, placements, and efficiency corrected absolute intensities (per 100 decay events) of transitions in ^{42}S from the β decay of ^{42}P decay.

E_γ (keV)	$E_i \rightarrow E_f$ (keV)	I (%)
903(1)	903 → 0	26.3(2.7)
1820(1)	2724 → 903	4.5(5)
2010(1)	5012 → 3003	7.3(8)
2100(1)	3003 → 903	5.0(6)
2493(2)	5494 → 3003	0.6(2)
2580(1)	3483 → 903	1.5(3)
2679(2)	3582 → 903	2.5(4)
2805(1)	3708 → 903	1.3(3)
2836(2)	5839 → 3003	0.7(3)
3003(1)	3003 → 0	8.1(9)
3708(2)	3708 → 0	<0.5
4110(2)	5012 → 903	2.6(4)
4243(2)	5146 → 903	1.0(2)
4591(1)	5494 → 903	5.1(7)
4936(2)	5839 → 903	1.8(4)

2. ^{43}P ($Z = 15$; $N = 28$)

^{43}P is proposed to have a $\frac{1}{2}^+$ ground state [35] because of the unpaired proton in the sd shell, and its β^- decay should feed $\frac{1}{2}^+$ and $\frac{3}{2}^+$ states in the daughter nucleus via GT transitions. ^{43}S has recently been studied several times [6,30,36,37] and confirmed to have a 320-keV $\frac{7}{2}^-$ isomeric excited state with $\frac{3}{2}^-$ as the ground state. This inversion is suggestive of the melting of the $N = 28$ shell gap as mentioned before. More recently, in a one-neutron knockout reaction from ^{44}S [37], several states with proposed negative parity have been identified along with a 2.6-MeV state with a likely $J^\pi = \frac{3}{2}^+$ assignment decaying directly to the ground state. It is purported to be the neutron knockout from the $0d_{3/2}$ orbital in ^{44}S. In β decay, this state can be formed by the transformation of the $0d_{3/2}$ neutron to $0d_{3/2}$ proton creating a core excited 1p1h state in an allowed GT transition. The low-lying $\frac{1}{2}^-$, $\frac{3}{2}^-$, and $\frac{5}{2}^-$ states in ^{43}S can also be populated via FF transition.

The β-delayed γ spectrum up to 100 ms after an implant is shown in the top panel of Fig. 6. The strongest transition seen is the 903 keV $2^+ \rightarrow 0^+ \gamma$ ray from ^{42}S formed through the $\beta 1n$ channel. No other γ transition with the same decay time as the 903-keV line is observed. Neither are any γ transitions from ^{41}S seen. This would imply that ^{43}P almost exclusively decays via the $\beta 1n$ channel, i.e., $P_n = 100\%$, as decay to the ground state is possible only by a weak FF transition. In the bottom panel of the figure the correlation time has been extended to 1000 ms to look for transitions in the granddaughter ^{43}Cl following the β decay of ^{43}S if produced. The inset shows the actual β-delayed γ ray spectrum of ^{43}S to ^{43}Cl (gating on the ^{43}S implants from the current data) where the 328- and 880-keV γ ray transitions are observed, representing the two lowest states in ^{43}Cl. In contrast, these two transitions are completely absent in the ^{43}P decay for the same correlation window (the arrows in the figure are guides to where the two peaks should have been), confirming that no ^{43}S was formed in its β decay. In the only earlier work to measure P_n value for ^{43}P [19], a value of 100% was measured by observing neutrons, and here we confirm it by a completely different approach. One of the reasons for the 100% βn decay is the low S_n value of 2629(9) keV in ^{43}S [31]. Still, it is surprising as a 2600 keV $3/2^+$ was observed in ^{43}S [37] and there are several negative-parity states below S_n which could have been populated in FF transitions.

Figure 7 shows the decay curve for ^{43}P for a correlation time window of 1000 ms. An excellent fit to the decay curve was obtained by excluding the decay of the $\beta 0n$ daughter ^{43}S consistent with our prior discussion on P_n being 100%. The $T_{1/2}$ thus obtained is 37.5(22) ms consistent with the evaluated value of 36.5(15) ms [18,31].

3. ^{44}P ($Z = 15$; $N = 29$)

We cross the $N = 28$ shell gap with ^{44}P and as already discussed for the odd-odd $N = 27$ isotope ^{42}P, the low-lying

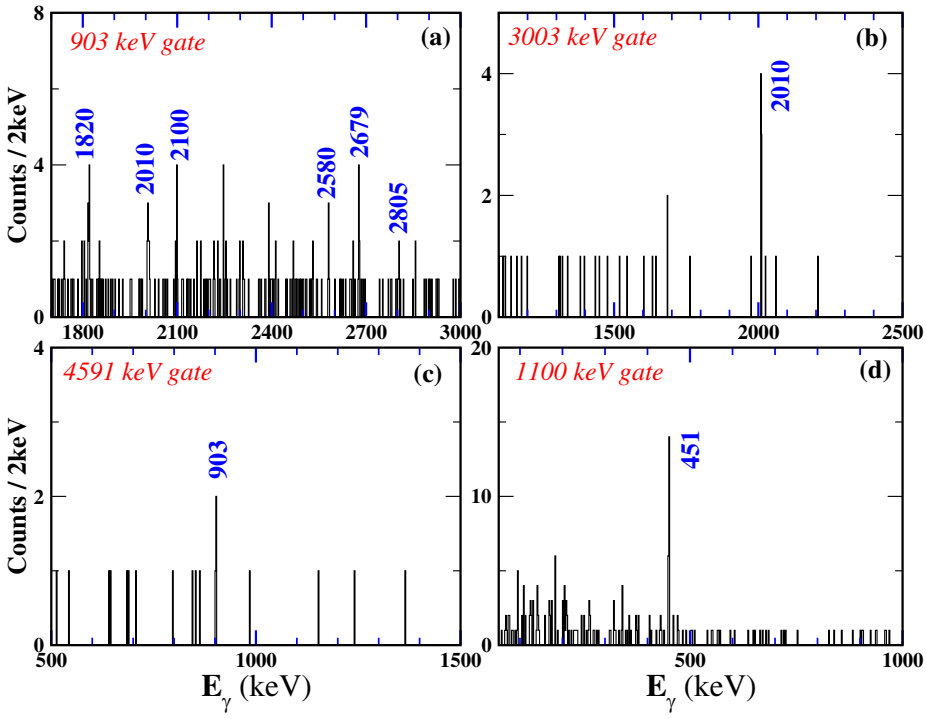

FIG. 3. [(a)–(c)] Coincidences observed between the γ transitions in ^{42}S. (d) Coincidence spectrum for ^{41}S with a gate on 1100 keV showing the 451-keV transition.

states are built on the $\pi d_{3/2}$-$\nu p_{3/2}$ configuration. Shell-model calculations [13,26] predict 0^- as the ground state from that configuration with the 1^- and 2^- lying close by. A half-life of 18.5(25) ms is known from the prior GANIL work [18], showing a drop of a factor of 2 from ^{43}P. Beyond that, no other experimental information exists for ^{44}P, though an extrapolation from ^{43}P would imply a P_n close to 100%.

The decay curve for ^{44}P is shown in Fig. 8 where a fit assuming 100% P_n gives an excellent reproduction of the data similar to ^{43}P with a half-life of the parent of 18(1) ms agreeing very well with the previous measurement as well as a SM calculation by Yoshida *et al.* [13,15]. Inclusion of a small $\beta 0n$ branch did not change the half-life beyond the error quoted. As was seen for ^{43}P, the $T_{1/2}$ extracted from the decay curve is not very sensitive to P_n value, likely because the half-lives of both $\beta 0n$ and $\beta 1n$ daughters are long compared to their parent.

Going beyond the decay curve, we look at the β-delayed γ spectrum for ^{44}P in Fig. 9. In the short correlation window, a weak 1330-keV transition is seen which represents the $2^+ \rightarrow 0^+$ of the $\beta 0n$ daughter, ^{44}S, and perhaps the 955-keV transition from the proposed 2^+ state at 2283 keV as seen in the inverse kinematics proton scattering [35]. No other transition is observed feeding these 2^+ states. There are no candidates for any strong decay from the negative-parity states at higher energies fed by allowed GT decay as were observed in ^{42}S.

On the other hand, the prominent 185- and 1155-keV transitions are from ^{43}S, the $\beta 1n$ daughter. The 1155-keV depopulates a state at the same energy with a likely J^π of $3/2^-$ as was observed in a neutron-knockout reaction [37] and in the same study the 185-keV transition was proposed to decay from the 1162-keV state to the 977-keV second $7/2^-$ state which decays to the ground state. The 977-keV state was verified in a recent Coulomb-excitation experiment [38]. As can be seen from Fig. 9 (top panel) we have very tentative indications of a 983-keV transition instead of 977 keV, if at all. However, the crucial point is that the 185-keV transition is stronger in contradiction to the neutron knockout experiment. In an earlier measurement to measure lifetimes [6], the order of the 977- and 185-keV transitions was proposed to be reversed; 977 keV depopulating the 1162-keV $(5/2^-)$ state to the 185-keV state with $J^\pi = 1/2^-$ and the 185-keV transition depopulating that. The current β-decay data seems to corroborate this ordering, which is also consistent with the SM predictions of a low-lying $1/2^-$ state. ^{44}P is proposed to have a 0^- ground state, feeding a 1^- neutron resonance which can emit an $\ell = 0$ neutron populating $\frac{1}{2}^-$ and $\frac{3}{2}^-$ states. If the J^π of the 1162-keV state is indeed $\frac{5}{2}^-$ as proposed, then it is less likely to be populated in the $\beta 1n$ decay if ^{44}P has a 0^- ground state but possible if it has higher spin for its ground state.

The γ spectrum when followed for 1000 ms after the initial implantation shows the transitions from $\beta 0n$ and $\beta 1n$ granddaughters, namely 2789 keV in ^{44}Cl (see next section) and 328 and 880 keV in ^{43}Cl. The lowest, 118-keV transition from ^{42}Cl is also observed with a rather small intensity implying

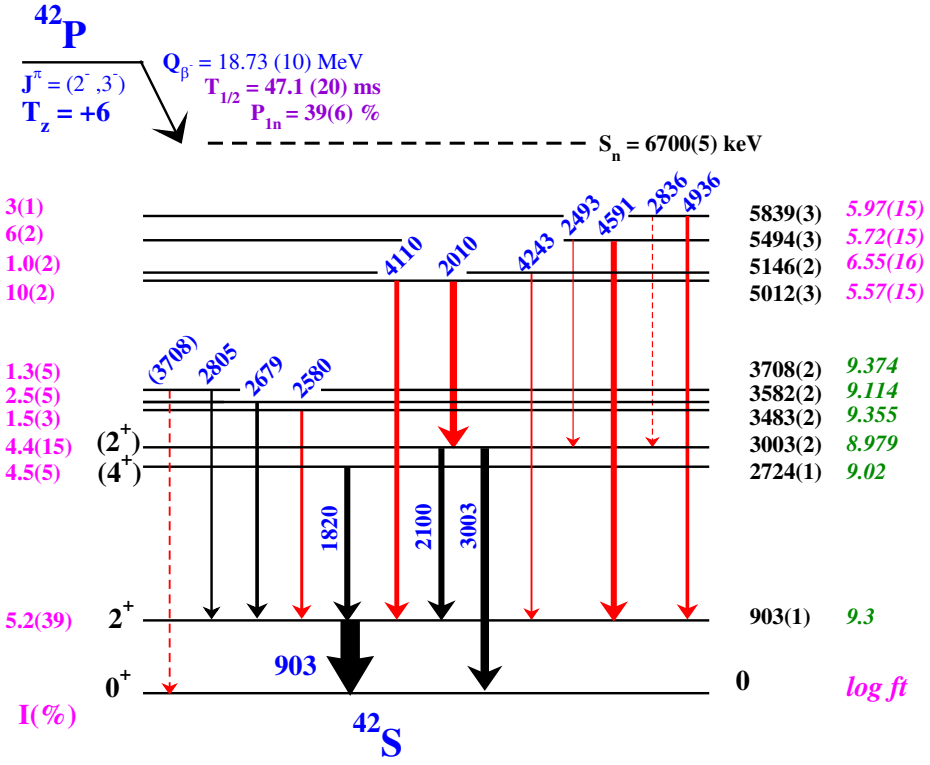

FIG. 4. Partial level scheme of ^{42}S following β decay of ^{42}P with a $T_{1/2} = 47.1(20)$ ms and $Q_{\beta^-} = 18.73(10)$ MeV. The transitions marked black were known before, whereas red indicates the new transitions. The absolute branching for each level was calculated using the measured yield in the gamma transition, total number of implants from the decay curve, and the γ detection. The width of the arrows are approximately proportional to the absolute intensity. The logft values were calculating using the logft calculator [31]. For levels above 5 MeV, they represent GT transitions while below indicate FF.

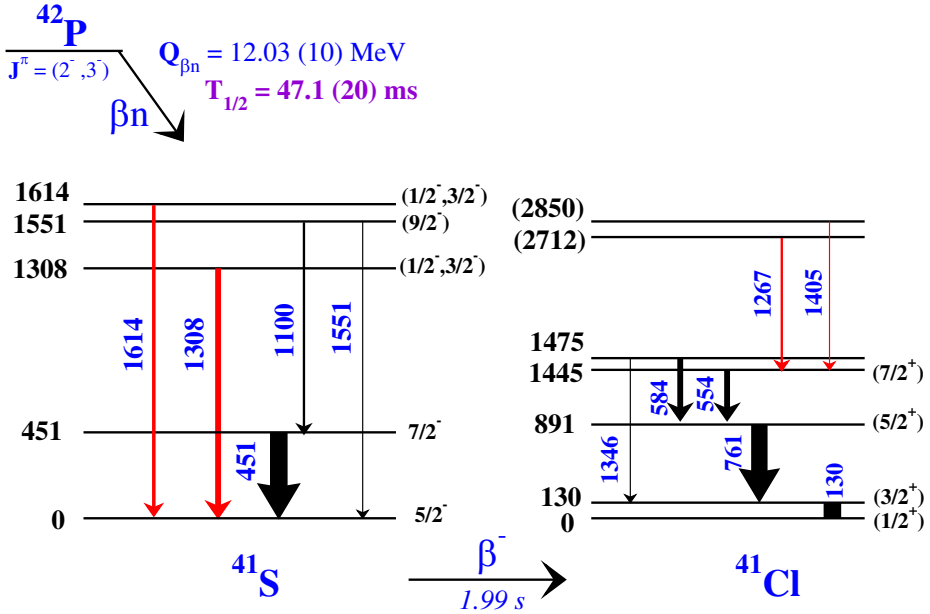

FIG. 5. Partial level scheme of β-delayed neutron daughter ^{41}S and granddaughter ^{41}Cl. The transitions in red have been confirmed in this work though they had been tentatively suggested before [31]. The arrow widths are only approximately proportional to intensity.

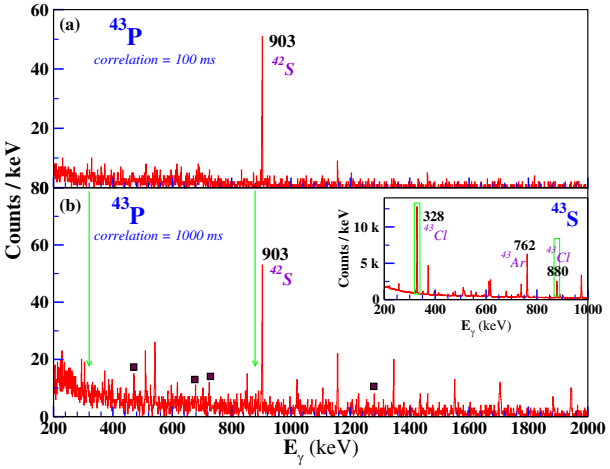

FIG. 6. (a) β-delayed γ spectrum for ^{43}P for a correlation time window of 100 ms. (b) The same for a correlation time window of 1000 ms to look for γ transitions in granddaughter nuclei. No γ transitions from ^{43}Cl are observed while the filled squares are transitions in ^{42}Cl. The inset shows the β decay of ^{43}S where the 328- and 880-keV γ rays are the two strongest γ transitions. (As mentioned in Sec. II, details of the ^{43}S decay will be discussed in detail in a forthcoming publication.)

that $\beta 2n$ is much weaker than $\beta 1n$. From the yields of the γ rays in the granddaughter nuclei, the P_n value is estimated to be 75(18)%.

B. Even-even S isotopes

The β^- decay of an even-even nucleus with a 0^+ ground state is special in that it is characterized by strong low-energy GT transitions to the odd-odd daughter nucleus. By that it is

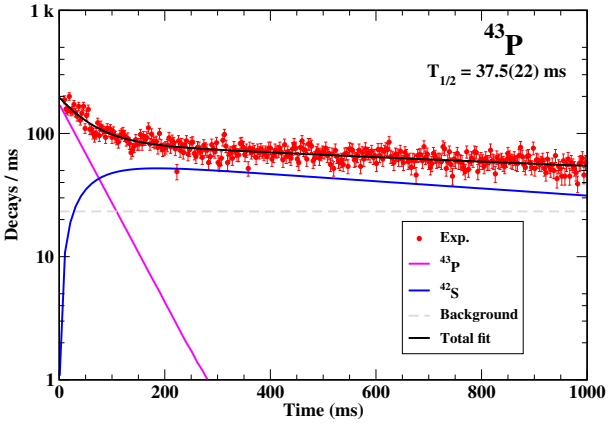

FIG. 7. Decay curve derived for ^{43}P from β-correlated implants within a grid of nine pixels shown for 1000 ms. An excellent reproduction of the decay curve is obtained by considering the exponential decay of ^{43}P along with exponential growth and decay of only the β-n daughter nuclei, ^{42}S, with a $T_{1/2}$ of 1016(15) ms [31] and a constant background.

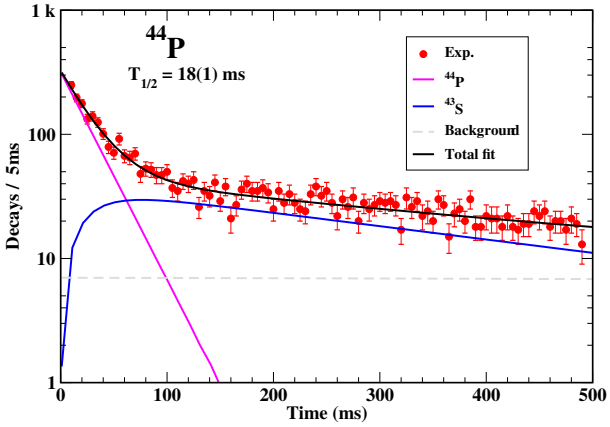

FIG. 8. The decay curve for ^{44}P and fitted in the same manner as ^{43}P.

implied that the B(GT) to a discrete state below roughly 5 MeV is >0.1 or a logft value <4.78 as discussed in Ref. [13]. As the allowed GT decay from the 0^+ parent will feed only 1^+ states, there exists a 1^+ state in the odd-odd daughter with a strong β transition strength. The neutron-proton pairing force in the $J^\pi = 1^+$ channel is responsible for lowering the energy of this 1^+ state. Yoshida *et al.* [13] demonstrate in their calculations that switching off the proton-neutron 1^+ pairing matrix greatly reduces the low-energy GT strength.

In ^{40}S and ^{42}S, β^- decay strong population of the 1^+ state around 2 MeV in the daughters (2306 keV in ^{40}Cl and 2123 keV in ^{42}Cl) is seen. It would be interesting to see how the

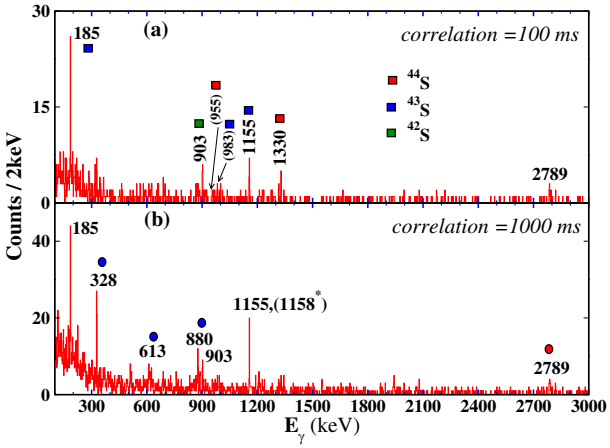

FIG. 9. β-delayed γ spectrum for ^{44}P (a) for a correlation window of 100 ms and (b) for 1000 ms. Transitions marked with red filled squares belong to $\beta 0n$ daughter ^{44}S and red circles are the $\beta 0n$ granddaughter ^{44}Cl. Blue filled squares are $\beta 1n$ daughter ^{43}S and blue circles $\beta 1n$ granddaughter ^{43}Cl, while green squares and circles are for the $\beta 2n$ daughter and granddaughter ^{42}S and ^{42}Cl. The * in (b) indicates there is a doublet comprising the 1155- and 1158-keV transitions where the 1158-keV transition is from the long activity in either ^{44}Ar or ^{44}K.

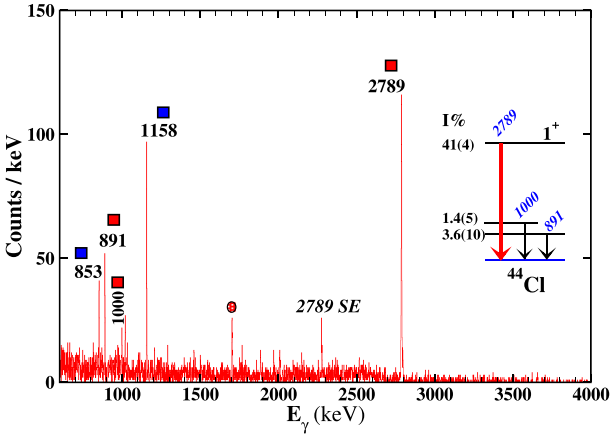

FIG. 10. β-delayed γ spectrum for a correlation window of 100 ms for ^{44}S decay. Red filled squares indicate transitions in ^{44}Cl while blue filled squares belong to ^{44}Ar. The 1703.4-keV transition (red shaded circle) belongs to ^{44}K and is a long lived activity found in all time windows. The absolute intensities of the 2789-, 1000-, and 891-keV transitions are 41(4)%, 1.4(5)%, and 3.6(10)% respectively.

low-energy GT strength evolves as a we move to more exotic neutron-rich nuclei and in turn give an idea of the proton-neutron paring strength when the proton and neutron occupy different shells. The β decay of ^{44}S and ^{46}S with neutron numbers 28 and 30, respectively, studied here for the first time with delayed γ rays, allowed us to explore this effect.

1. ^{44}S *($Z = 16$; $N = 28$)*

The delayed γ spectrum for the ^{44}S implants, 100 ms after the implantation, is shown in Fig. 10. The strongest transition observed is at 2789(1) keV with a half-life consistent with ^{44}S decay as will be discussed next. The single escape peak of this transition was also seen and is indicated in the spectrum. The 2789-keV transition is proposed to depopulate a level at the same energy as no coincidences are observed and based on prior discussion would correspond to the 1^+ state in ^{44}Cl populated strongly by allowed GT transitions. This follows the trend of the lighter isotopes of a strong low-lying 1^+ state in the daughter nucleus, though the energy is higher than in ^{42,40}Cl. Also seen in the spectrum are weak transitions at 891 and 1000 keV which have previously been tentatively assigned to ^{44}Cl [39]. Here they would be populated through FF decay as the 1^+ intruder 1p1h states are predicted around 3 MeV. These states at 891 and 1000 keV are good candidates for the calculated 0_1^- (844 keV), 1_2^- (1047 keV), and 0_2^- (1378 keV) or 2_2^- (971 keV) states which would decay directly to the 2^- ground state of ^{44}Cl and their intensity (1–2%) is consistent with the logft values calculated for the FF decays [15]. The other lower-lying states seen in [39] are not observed here. Also seen are the lowest transitions in the granddaughter ^{44}Ar (1158 and 853 keV). Out of scale in the figure is the 328-keV transition from ^{43}Cl, the $\beta 1n$ daughter. The P_n value is estimated to be 40(5)%, based on the γ intensity observed in the descendants and is consistent with intensity found for the bound states in ^{44}Cl.

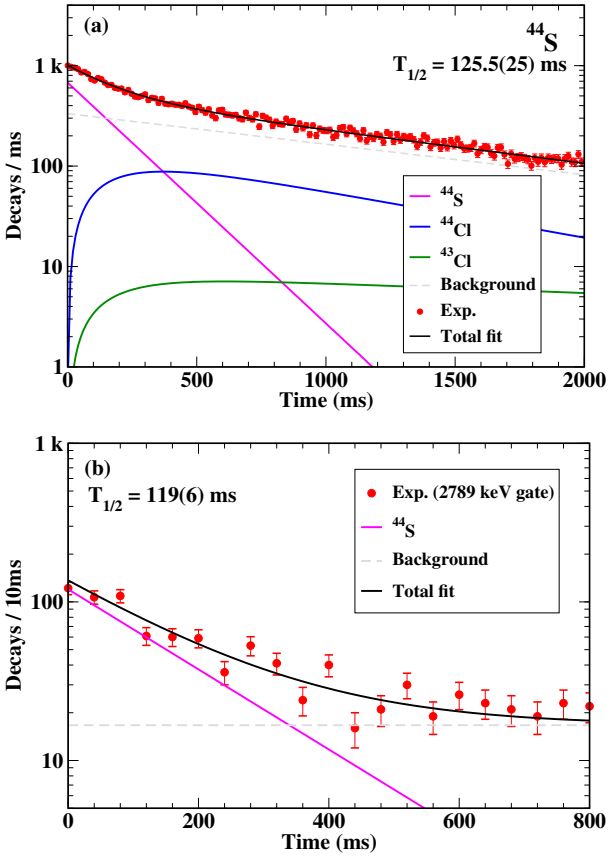

FIG. 11. (a): Decay curve derived for ^{44}S from β-correlated implants within a grid of nine pixels for 2s along with the fit used to extract half-life and the initial activity. The components of the fit are (i) exponential decay of parent, ^{44}S, (ii) exponential growth and decay of daughter nuclei, ^{44}Cl (β 0n) and ^{43}Cl (β 1n), and (iii) exponential background. Known half-lives were used for the daughter nuclides [31]. (b): Decay curve gated by the 2789-keV transition which represents the $1^+ \rightarrow 2^-$ in $\beta 0n$ daughter ^{44}Cl.

The decay curves for ^{44}S implants and with the additional gate of the 2789-keV γ transition are shown in Fig. 11. The extracted half-lives are 125.5(25) and 119(6) ms, respectively. The two previous measurements were 100(1) ms [18] and 123(10) ms [19] and our measurement supports the longer half-life. The SM calculation by Yoshida *et al.* [13] gives 121.3 ms as the half-life, in excellent agreement with the measurement.

2. ^{46}S *($Z = 16$; $N = 30$)*

^{46}S with $N = 30$ is the most exotic isotope produced and studied in this experiment. Grevy *et al.* [18] earlier measured its half-life to be 50(8) ms with no further information. The first and only study of the excited levels of the $\beta 0n$ daughter ^{46}Cl was via fragmentation of ^{48}K where two low-lying states at 118 and 151 keV were clearly identified [39] though no spin/parity assignment could be made.

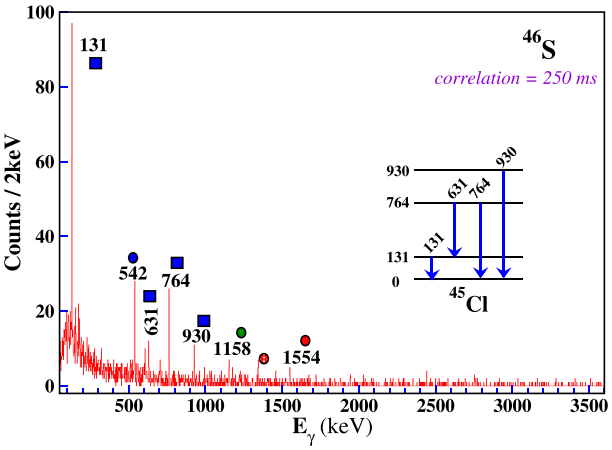

FIG. 12. β-delayed γ spectrum for a correlation window of 250 ms for ^{46}S decay. The four transitions from ^{45}Cl are marked by blue filled squares while blue filled circles are those from ^{45}Ar. The 1554-keV transition represents the $2^+ \rightarrow 0^+$ transition in ^{46}Ar. The 1346 keV is the $2^+ \rightarrow 0^+$ in ^{46}Ca and is a long lived activity.

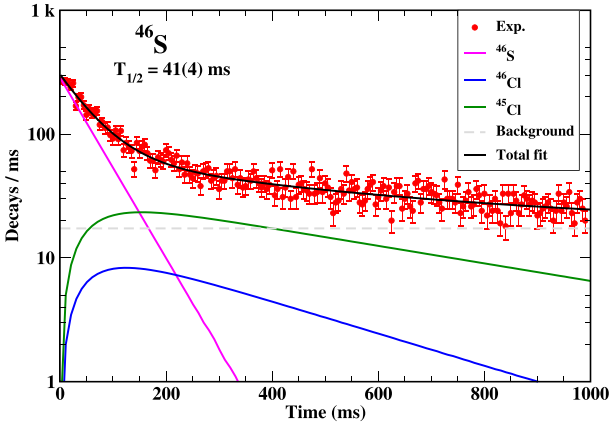

FIG. 13. Decay curve derived for ^{46}S from β-correlated implants within a grid of nine pixels for 1s along with the fit used to extract half-life and the initial activity. The components of the fit are (i) exponential decay of parent, ^{46}S, (ii) exponential growth and decay of daughter nuclei, ^{46}Cl (β0n) and ^{45}Cl (β1n), and (iii) constant background. Known half-lives were used for the daughter nuclides [31].

The β-delayed γ spectrum for ^{46}S is shown in Fig. 12. The strongest and clearest transitions marked by blue squares belong to ^{45}Cl which is the $\beta 1n$ daughter as illustrated by the cartoon in the figure. The spectrum is shown for a correlation window of 250 ms and in that time one can also see the transitions from the $\beta 1n$ granddaughter, ^{45}Ar, namely 542 and 1158 keV. Unlike the decay of ^{44}S, no strong transition is observed which can be associated with the decay of the 1^+ state likely to be populated in the GT decay of 0^+ parent. This illustrates that for $N = 30$, the states populated by GT transitions have moved above the 3.5-MeV neutron separation energy (S_n) limit and lie among the neutron unbound states leading to strong delayed neutron emission. The weak 1554-keV transition observed corresponds to the $2^+ \rightarrow 0^+$ decay in ^{46}Ar, the β0n daughter. Though the β decay of ^{46}Cl is not reported, if we assume that the 1554-keV transition is indeed from this path, then there must be a bound state populated in ^{46}Cl, albeit weakly, which cannot be isolated in the current data. It is thus clear that the GT strength has moved above the neutron threshold, and ^{46}S, though an even-even isotope, does not display the strong low-energy GT strength as was expected in Ref. [13].

The decay curve for ^{46}S, shown in Fig. 13, was used to extract a half-life of 41(4) ms. Though smaller than the literature value of 50(8) ms [18], it is quite consistent with the shell-model prediction discussed earlier. The contribution of the $\beta 0n$ and $\beta 1n$ daughter were allowed to vary for this fit and the best reproduction of the decay curve is consistent with a large P_n value. A $\beta 2n$ contribution was not included as no γ transitions from the $\beta 2n$ daughter or granddaughter were seen. The P_n value is estimated to be 80(16)% for this case.

C. Discussion

As we know, β decay is a well-established probe of nuclear structure; with the half-lives providing the first insight. The $N = 28$ isotones below ^{48}Ca are characterized by large deformation and shape coexistence, in spite of the shell closure which should be reflected in the measured half-lives. The shell-model calculations using the SDPFSDG-MU interaction in the large $sd + fp + sdg$ valence space reproduce the properties of these exotic nuclei quite well with the oblate deformation of ^{42}Si and shape coexistence in ^{44}S. In Refs. [13,15], Yoshida *et al.* carried out calculations of β^--decay half-lives and β-delayed neutron emission probabilities using this interaction for neutron-rich nuclei with $13 \leqslant Z \leqslant 18$ and $22 \leqslant N \leqslant 34$. The half-lives were calculated in two conditions, one when only GT transitions were allowed and then also including the FF transitions (GT+FF) both using experimental Q_{β^-} values.

The measured half-lives of P and S isotopes are compared to the calculations in the two scenarios in Fig. 14 and Table II.

TABLE II. Comparison of the measured half-lives ($T_{1/2}$) and SM predictions discussed in the text [15] for the P and S isotopes studied in this work

	Expt.		SM		
Nuclide	$T_{1/2}$ (ms) (no γ)	$T_{1/2}$ (ms) γ-gated	J^π (E^*)	$T_{1/2}$ (ms) GT+FF	$T_{1/2}$ (ms) GT only
^{42}P	47.1(20)	49.5(25)	0^- (0 MeV)	36.982	55.969
			1^- (0.13 MeV)	44.198	56.085
			2^- (0.19 MeV)	53.294	61.616
			3^- (0.29 MeV)	60.898	64.127
			4^- (0.41 MeV)	66.198	68.429
^{43}P	37.5(22)	–	$1/2^+$ (0 MeV)	28.337	31.709
^{44}P	18(1)	–	0^- (0 MeV)	16.643	21.597
			1^- (0.27 MeV)	18.026	23.872
			2^- (0.35 MeV)	24.700	29.081
^{44}S	125.5(25)	119(6)	0^+ (0 MeV)	121.273	129.352
^{46}S	41(4)	–	0^+ (0 MeV)	36.808	40.536

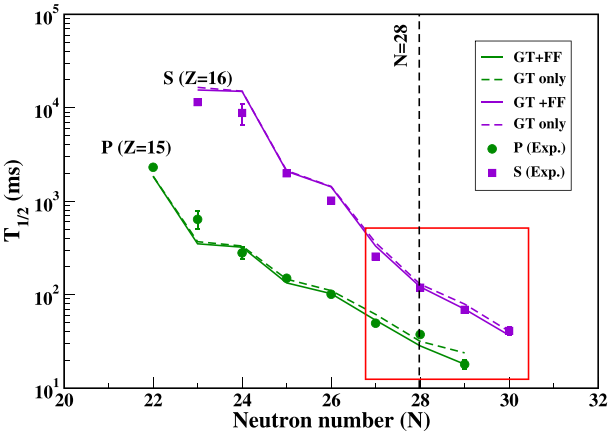

FIG. 14. Comparison of measured $T_{1/2}$ values for P and S isotopes from $N = 22$ to $N = 30$ with shell-model calculations using the SDPFSDG-MU interaction [13]. The numbers in the red box are from the current data set while others are the evaluated values from NNDC [31].

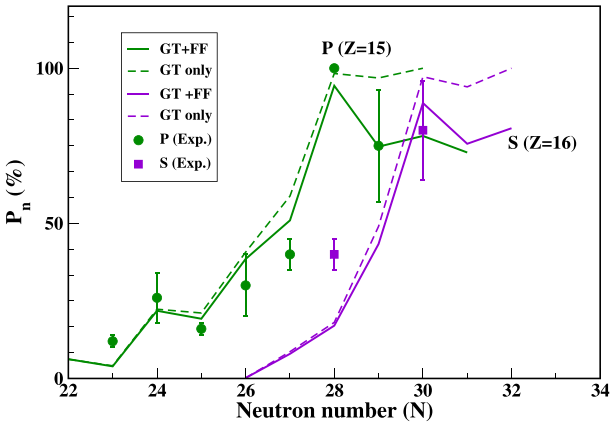

FIG. 15. Comparison of experimental P_n values for P and S isotopes from $N = 22$ to $N = 30$ with shell-model calculations using the SDPFSDG-MU interaction [13]. The numbers extracted in the current analysis are augmented with values from NNDC.

The numbers within the red box are those from the current work, while the rest are the evaluated values from NNDC [31]. The half-lives of the odd-N nuclei, ^{43,45}S, were not discussed here but will be part of a forthcoming publication. As can be seen, there is not much difference between the GT only and GT+FF predictions both for P and S isotopes, and the measured and calculated numbers agree fairly well except for the most exotic ^{44}P. For both calculations, experimental $Q(\beta^-)$ values were used from the AME2016 database when measured; for the most exotic ^{44}P and ^{46}S the numbers are from systematic trends. Not using the experimental $Q(\beta^-)$ for the calculation systematically underestimates the half-lives by about 66% on average. For the $N = 27$ nucleus ^{42}P, using different ground-state spins (0^- to 4^-) gives divergent answers with the favored 0^- possibility giving the lowest value of ≈37 ms which is not consistent with the measurement. The decrease is primarily due to the small logft value of the ground-state-to ground-state FF decay. In Fig. 14 we show the value corresponding to the 2^- as ground-state spin which gives the overall best reproduction of the data. For the $N = 28$ nucleus ^{43}P for which we determined a 100% P_n value, the measured half-life is longer by about 30% from the calculated value including FF but there is better agreement for ^{44}P when considering the FF transitions. It is also noticeable that for ^{42}P ($N = 27$) and ^{43}P ($N = 28$), the measured half-lives are very close and then fall by a factor of 2 for ^{44}P, whereas for the equivalent S isotopes there is a smooth trend. This could signal a somewhat larger $N = 28$ shell closure for P than S. There is enough evidence already to suggest that the $N = 28$ gap is completely quenched for the S isotopes.

The measured β-delayed neutron emission probabilities, P_n, for the P and S isotopes are also compared to the above-mentioned SM calculations with both GT only and GT+FF estimates in Fig. 15. The measured values track the calculation well especially for the odd Z P isotopes which display a higher P_n for the same neutron number. For the $N = 28$ isotope ^{43}P, 100% of the β decay proceeds via the delayed neutron path; for ^{44}S ($N = 28$) the P_n value is of the order of 40% only. This difference is due to the strong low-energy GT transition for the decay of the even-even S isotope. The 100% P_n for ^{43}P is predicted for GT only while it is somewhat less for GT+FF calculations. For ^{44}P the measured value is explained with the inclusion of FF which is consistent with the observation of the low-lying positive-parity states in ^{44}S (consistent with the half-life discussion). For the $N \geqslant 28$ nuclei in the shell-model calculations, some low-lying FF matrix elements are enlarged, thus contributing substantially to the total half-lives and reducing the delayed neutron emission. This is mainly attributed to the neutron Fermi surface moving to the $1p$ orbitals.

The disappearance of the $N = 28$ shell gap and the appearance of exotic shape coexistence can be correlated with the changed Fermi level for protons and neutrons as a function of deformation. In antisymmetrized molecular dynamics (AMD) calculations by Y. Suzuki and M. Kimura [40], it is shown that for prolate deformation, as found in exotic S isotopes with $N = 26$ to 30, the neutron Fermi level is the $1p_{3/2}$ orbital while for proton it is the $1s_{1/2}$ orbital. This will greatly enable the FF β transitions to occur. The half-lives and P_n values which are bulk β-decay properties already showcase the influence of FF decay but, additionally, we can specifically look for the states populated in these decays. We review the ^{42}P decay as was shown in Fig. 4. The detailed level scheme is based on energy and intensity balance and coincidences where possible. The logft values were deduced using the measured branching, $T_{1/2}$, and the Q_{β^-} from NNDC. As for the S isotopes, it is expected the 27$^{\text{th}}$ neutron is in the $1p_{3/2}$ orbital while the last proton is in the $0d_{3/2}$ orbital leading to a favored 0^- ground state in the SM calculations using the SDPFSDG-MU interaction [13,15] and also using the SDPF-U interaction [26]. However, other J^π combinations from the same configuration (0^- to 3^-) lie very close in energy and as we saw the measured half-life aligns better with higher spin assignment. The states observed in ^{42}S above 5 MeV have logft values which fall in the range for allowed GT transitions

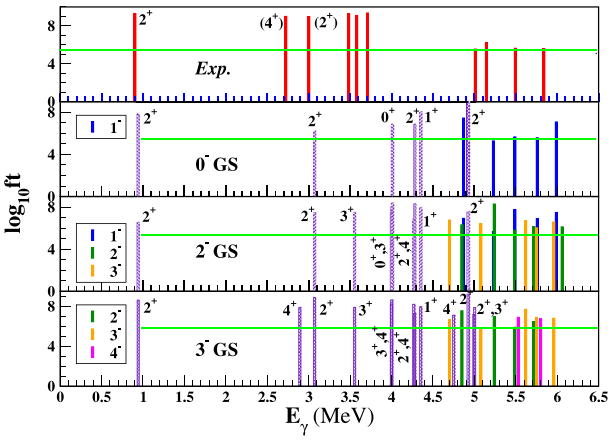

FIG. 16. Comparison of experimental energies and logft values for the decay of ^{42}P with SM calculations using the SDPFSDG-MU interaction [12,13,15]. Top panel is the experimental data while the three panels below are SM predictions for states populated in daughter nucleus ^{42}S with different assumptions of the ground state spin of ^{42}P with the same negative parity. The green horizontal line in each panel is just a marker of a logft value of 5.6. Both negative- and positive-parity states, which will be populated via GT and FF transitions, respectively, are shown. See text for further discussion on the comparison.

and hence should have negative parity as the odd-odd parent has a negative-parity ground state. All of them decay to the 2^+_1 and 2^+_2 states likely via $E1$ transitions. The absence of direct decay to the 0^+ ground state of ^{42}S makes it less likely that the populated states are of 1^- spin. Hence the assignment of 0^- to the ground state of ^{42}P is also unlikely.

In a recent intermediate-energy Coulomb-excitation study [38], a 4150(110)-keV transition was observed in coincidence with the 903-keV γ transition and a 2^+ state at 5050 keV was proposed with the same uncertainty. Though close in energy to the 5012-keV state in this work, we think they are different as we also observe the decay to the 2^+_2 state at 3003 keV and more so the large β branching to it makes it a candidate for a negative-parity state via GT decay. However because of the large error bars quoted for the 5050-keV level it could correspond to the 5146-keV that we observe with a weak branching and a decay to the 2^+_1 state only. If so, then it could be fed directly through FF for a 2^+ assignment to that state. The states just above 3 MeV, i.e., 3483, 3582, and 3708 keV, could also be candidates for FF decays as they are not likely to be the negative-parity 1p1h states. The 2724-keV level has already been assigned a 4^+ while the 3003-keV state has been earlier proposed to be a 2^+ state and is consistent with the SM predictions.

Figure 16 compares the experimental logft values with the SM predictions for the β^- decay of ^{42}P with different ground state possibilities (0^-, 2^-, 3^-). In the calculations the yrast 0^- to 4^- in ^{42}P are very close and one cannot predict definitely the actual ground state. The predicted decay from the 0^- ground-state gives several 1^- states as excellent candidates for the states observed above 5 MeV with logft values consistent with the experimental values; however, as noted before the decay of the states merely to the 2^+ states makes it a less likely possibility. Both the decay from 2^- and 3^- states also gives many 2^- and 3^- candidates in the energy range of 5 to 6 MeV with logft values consistent with the measurement. These can decay to the lower 2^+ states and likely not to the 0^+ ground state of ^{42}S. There are also candidates for the states below 5 MeV via FF decays; in particular, a 3^- ground state could feed the 4^+ state also via a FF decay. The apparent feeding observed to the states around and below 3 MeV of a few percentages is consistent with the predicted logft [15] values. Thus based on the current work we propose either 2^- or 3^- as the spin and parity of the ground state of ^{42}P. The population of higher spin states in the $\beta 1n$ channel (Fig. 5) also favors a higher than 0 spin for the ^{42}P ground state.

Next we look at the systematics of the decay of the even-even S isotopes and the predictions for the SDPFSDG-MU interaction in that regard. Shown in Fig. 17 are the partial level schemes as populated in the GT allowed decay of ^{40,42,44,46}S. The even-even parent (0^+) nucleus in all cases is expected to strongly populate the 1^+ states in odd-odd Cl isotopes that have large B(GT) values via GT transitions [13]. The spin-isospin component of the NN interaction may favor proton-neutron pairs in the daughter nucleus, created by the action of the GT operator on a BCS-type neutron-neutron pair contained in the ground state of the parent nucleus. The trend of the 1^+ states to move to higher energies as the neutron number increases is reproduced by the SM calculation, where for ^{46}Cl the strong GT branches with small logft values lie above the neutron separation energy. Coupling this to the lowering of the neutron separation energy S_n with increasing neutron excess and the P_n value makes a rapid change from ^{44}S to ^{46}S, reaching almost 100%. As noted earlier, in ^{44}S decay, we did observe weak population of low-lying negative-parity states in ^{44}Cl. A significantly larger contribution of FF will further reduce the P_n and it would be interesting to see what will be the case for the next exotic even-even S isotope, ^{48}S, which is yet to be observed and studied.

Also, we should note that the SM predictions for ^{44}S decay are two states, 1^+_3 and 1^+_4 (i.e., the third and fourth in energy), which have small logft values. The energies of the two are very close and have nearly equal logft with either being a good candidate of the experimentally observed state. Examining the occupancies of the two states from the calculations in comparison to those of the ground state of parent ^{44}S reveals that the 1^+_3 state is formed predominantly by the transformation of the sd neutrons to sd protons, namely $\nu 1s_{1/2}$ to $\pi 1s_{1/2}$ and $\nu 0d_{3/2}$ to $\pi 0d_{3/2}$. For the 1^+_3 it is the transformation of the fp neutrons which is the dominant component. It is difficult to determine which of these we are not observing. A second state with a similar logft decaying to the ground state (like the 2789 keV) should have been measurable. It is likely then that one of them is higher in energy and above S_n which would be consistent with a higher P_n value observed than what the SM predicts for ^{44}S (Fig. 15).

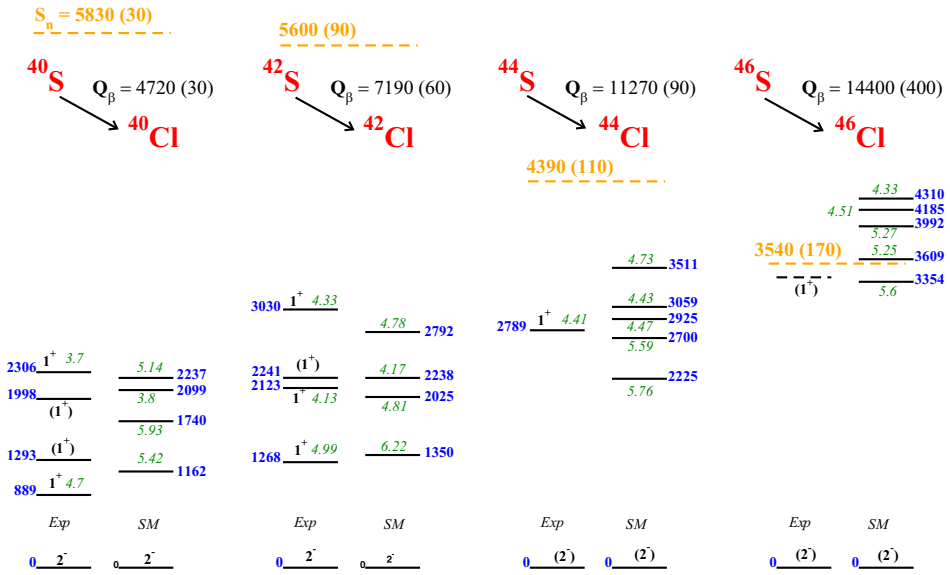

FIG. 17. β decay of even-even S isotopes from $A = 40$ to 46. Data for ^{40,42}S are from NNDC [31]. Only the 1^+ states expected to be populated via allowed GT transitions along with SM prediction are shown. As mentioned in the text we could not isolate the weakly populated bound 1+ state in ^{46}Cl. The focus is to illustrate that with increasing neutron number the GT strength imbibed by the 1^+ states moves to higher energies eventually residing in the neutron unbound states for ^{46}S.

IV. SUMMARY

β^- decay of very exotic P and S isotopes reaching and beyond the $N = 28$ shell gap were studied at the NSCL using a 40×40 DSSD as the implant and β detector, surrounded by a γ array of 16 Clover detectors in close geometry. The half-lives were extracted from the fitting of decay curves for $^{42-44}$P and ^{44,46}S and are mostly consistent with the earlier work from GANIL, except for ^{44}S, which at 125.5(25) ms is somewhat longer than the literature value of 100(1) ms and ^{46}S which is smaller than previously measured. The P_n values were also calculated, and for ^{43}P decay we have a case of 100% P_n, and for both ^{44}P and ^{46}S, with $N = 29$ and 30 respectively, it is reaching 100%, too. The impact of FF transitions which can be important for neutron-rich nuclei in this region with neutrons filling the $1p_{3/2}$ orbital was explored by comparing the measured $T_{1/2}$ and P_n values with SM calculations with and without FF transitions included. The P isotopes with $N = 27, 28, 29$ displayed a larger contribution from FF transitions in their β decay. For the case of ^{42}P decay there are clear indicators of states which could be populated in FF decay with logft values consistent with the predictions of the SM calculations. Both the half-life and P_n value of ^{44}P also indicate influence of FF transitions. Comparison with SM calculations of states populated in ^{42}S in the decay of ^{42}P both via allowed GT and FF decays suggests a J^π of 2^- or 3^- for the ground state of ^{42}P contrary to earlier suggestion of 0^-. Further, for the even-even S isotopes studied, ^{44,46}S, the predicted strong low-energy GT strength is observed for ^{44}S with a 1^+ state strongly populated at 2789 keV. On the other hand, for ^{46}S the 1^+ states move higher in energy and lie above S_n, leading to a large P_n value. These interesting systematics for P and S isotopes with neutron number close to 28 are crucial for refining the calculations in this exotic region and set the stage for more detailed studies of the even more exotic nuclei to be explored at the Facility for Rare Isotope Beams (FRIB) in the coming months and years.

ACKNOWLEDGMENTS

We thank the NSCL operation team and the A1900 team, and especially Tom Ginter, for the production and optimization of the secondary beam. Help from Diya Choudhary and Wonmin Song, undergraduate students at FSU, in the fitting of the decay curves and insightful discussions with A. Volya (FSU) are acknowledged. This work was supported by the U.S. National Science Foundation under Grants No. PHY-2012522 (FSU) and No. PHY-1848177 (CAREER); U.S. Department of Energy, Office of Science, Office of Nuclear Physics under Awards No. DE-SC0020451 (FRIB), No. DE-FG02-94ER40848 (UML), No. DE-AC52-07NA27344 (LLNL), and No. DE-AC02-06CH11357(ANL) DE-SC0014448 (Mississippi State); the U.S. Department of Energy (DOE) National Nuclear Security Administration Grant No. DOE-DE-NA0003906; and the Nuclear Science and Security Consortium under Award No. DE-NA0003180. Y.U. and N.S. acknowledge JSPS KAKENHI Grants No. 20K03981 and No. 17K05433, "Priority Issue on post-K computer" (hp190160 and hp180179), and "Program for Promoting Research on the Supercomputer Fugaku" (hp220174 and hp210165). S.Y. acknowledges JSPS KAKENHI Grant No. 22K14030 for supporting this work.

[1] S. Calinescu, L. Cáceres, S. Grévy, O. Sorlin, Z. Dombrádi, M. Stanoiu, R. Astabatyan, C. Borcea, R. Borcea, M. Bowry, W. Catford, E. Clément, S. Franchoo, R. Garcia, R. Gillibert, I. H. Guerin, I. Kuti, S. Lukyanov, A. Lepailleur, V. Maslov *et al.*, Phys. Rev. C **93**, 044333 (2016).

[2] J. J. Parker, I. Wiedenhöver, P. D. Cottle, J. Baker, D. McPherson, M. A. Riley, D. Santiago-Gonzalez, A. Volya, V. M. Bader, T. Baugher, D. Bazin, A. Gade, T. Ginter, H. Iwasaki, C. Loelius, C. Morse, F. Recchia, D. Smalley, S. R. Stroberg, K. Whitmore *et al.*, Phys. Rev. Lett. **118**, 052501 (2017).

[3] T. Glasmacher, B. Brown, M. Chromik, P. Cottle, M. Fauerbach, R. Ibbotson, K. Kemper, D. Morrissey, H. Scheit, D. Sklenicka, and M. Steiner, Phys. Lett. B **395**, 163 (1997).

[4] T. Otsuka, A. Gade, O. Sorlin, T. Suzuki, and Y. Utsuno, Rev. Mod. Phys. **92**, 015002 (2020).

[5] O. Sorlin and M.-G. Porquet, Prog. Part. Nucl. Phys. **61**, 602 (2008).

[6] T. Mijatović, N. Kobayashi, H. Iwasaki, D. Bazin, J. Belarge, P. C. Bender, B. A. Brown, A. Dewald, R. Elder, B. Elman, A. Gade, M. Grinder, T. Haylett, S. Heil, C. Loelius, B. Longfellow, E. Lunderberg, M. Mathy, K. Whitmore, and D. Weisshaar, Phys. Rev. Lett. **121**, 012501 (2018).

[7] N. Tsunoda, T. Otsuka, K. Takayanagi, N. Shimizu, T. Suzuki, Y. Utsuno, S. Yoshida, and H. Ueno, Nature (Lond.) **587**, 66 (2020).

[8] A. Gade, B. A. Brown, D. Bazin, C. M. Campbell, J. A. Church, D. C. Dinca, J. Enders, T. Glasmacher, M. Horoi, Z. Hu, K. W. Kemper, W. F. Mueller, T. Otsuka, L. A. Riley, B. T. Roeder, T. Suzuki, J. R. Terry, K. L. Yurkewicz, and H. Zwahlen, Phys. Rev. C **74**, 034322 (2006).

[9] E. Caurier, F. Nowacki, and A. Poves, Phys. Rev. C **90**, 014302 (2014).

[10] M. Madurga, S. V. Paulauskas, R. Grzywacz, D. Miller, D. W. Bardayan, J. C. Batchelder, N. T. Brewer, J. A. Cizewski, A. Fijałkowska, C. J. Gross, M. E. Howard, S. V. Ilyushkin, B. Manning, M. Matoš, A. J. Mendez, K. Miernik, S. W. Padgett, W. A. Peters, B. C. Rasco, A. Ratkiewicz *et al.*, Phys. Rev. Lett. **117**, 092502 (2016).

[11] V. Tripathi, R. S. Lubna, B. Abromeit, H. L. Crawford, S. N. Liddick, Y. Utsuno, P. C. Bender, B. P. Crider, R. Dungan, P. Fallon, K. Kravvaris, N. Larson, A. O. Macchiavelli, T. Otsuka, C. J. Prokop, A. L. Richard, N. Shimizu, S. L. Tabor, A. Volya, and S. Yoshida, Phys. Rev. C **95**, 024308 (2017).

[12] Y. Utsuno, T. Otsuka, B. A. Brown, M. Honma, T. Mizusaki, and N. Shimizu, Phys. Rev. C **86**, 051301(R) (2012).

[13] S. Yoshida, Y. Utsuno, N. Shimizu, and T. Otsuka, Phys. Rev. C **97**, 054321 (2018).

[14] A. Gottardo, D. Verney, I. Deloncle, S. Péru, C. Delafosse, S. Roccia, I. Matea, C. Sotty, C. Andreoiu, C. Costache, M.-C. Delattre, A. Etilé, S. Franchoo, C. Gaulard, J. Guillot, F. Ibrahim, M. Lebois, M. MacCormick, N. Marginean, R. Marginean *et al.*, Phys. Lett. B **772**, 359 (2017).

[15] S. Yoshida, Database (beta decay), https://github.com/sotayoshida/betadecaydataprc97.054321 (2022).

[16] E. Warburton, J. Becker, B. Brown, and D. Millener, Ann. Phys. **187**, 471 (1988).

[17] T. Marketin, L. Huther, and G. Martínez-Pinedo, Phys. Rev. C **93**, 025805 (2016).

[18] S. Grévy, J. Angélique, P. Baumann, C. Borcea, A. Buta, G. Canchel, W. Catford, S. Courtin, J. Daugas, F. de Oliveira, P. Dessagne, Z. Dlouhy, A. Knipper, K. Kratz, F. Lecolley, J. Lecouey, G. Lehrsenneau, M. Lewitowicz, E. Liénard, S. Lukyanov *et al.*, Phys. Lett. B **594**, 252 (2004).

[19] O. Sorlin, Z. Dombrádi, D. Sohler, F. Azaiez, J. Timár, Yu.-E. Penionzhkevich, F. Amorini, D. Baiborodin, A. Bauchet, F. Becker, M. Belleguic, C. Borcea, C. Bourgeois, Z. Dlouhy, C. Donzaud, J. Duprat, L. Gaudefroy, D. Guillemaud-Mueller, F. Ibrahim, M. J. Lopez *et al.*, Eur. Phys. J. A **22**, 173 (2004).

[20] O. Sorlin, D. Guillemaud-Mueller, R. Anne, L. Axelsson, D. Bazin, W. Böhmer, V. Borrel, Y. Jading, H. Keller, K.-L. Kratz, M. Lewitowicz, S. Lukyanov, T. Mehren, A. Mueller, Y. Penionzhkevich, F. Pougheon, M. Saint-Laurent, V. Salamatin, S. Shoedder, and A. Wöhr, Nucl. Phys. A **583**, 763 (1995).

[21] M. Birch, B. Singh, I. Dillmann, D. Abriola, T. Johnson, E. McCutchan, and A. Sonzogni, Nucl. Data Sheets **128**, 131 (2015).

[22] A. Gade and B. Sherill, Phys. Scr. **91**, 053003 (2016).

[23] D. Morrissey, B. Sherrill, M. Steiner, A. Stolz, and I. Wiedenhoever, Nucl. Instrum. Methods Phys. Res., Sect. B **204**, 90 (2003).

[24] J. Prisciandaro, A. Morton, and P. Mantica, Nucl. Instrum. Methods A **505**, 140 (2003).

[25] C. Prokop, S. Liddick, B. Abromeit, A. Chemey, N. Larson, S. Suchyta, and J. Tompkins, Nucl. Instrum. Methods A **741**, 163 (2014).

[26] L. Gaudefroy, Phys. Rev. C **81**, 064329 (2010).

[27] C. Nesaraja and E. McCutchan, Nucl. Data Sheets **133**, 1 (2016).

[28] J. Chen and B. Singh, Nucl. Data Sheets **135**, 1 (2016).

[29] M. Lewitowicz, Y. E. Penionzhkevich, A. Artukh, A. Kalinin, V. Kamanin, S. Lukyanov, N. Hoai Chau, A. Mueller, D. Guillemaud-Mueller, R. Anne, D. Bazin, C. Détraz, D. Guerreau, M. Saint-Laurent, V. Borrel, J. Jacmart, F. Pougheon, A. Richard, and W. Schmidt-Ott, Nucl. Phys. A **496**, 477 (1989).

[30] E. Lunderberg, A. Gade, V. Bader, T. Baugher, D. Bazin, J. S. Berryman, B. A. Brown, D. J. Hartley, F. Recchia, S. R. Stroberg, D. Weisshaar, and K. Wimmer, Phys. Rev. C **94**, 064327 (2016).

[31] NNDC https://www.nndc.bnl.gov/nudat3/

[32] S. Szilner, L. Corradi, F. Haas, G. Pollarolo, L. Angus, S. Beghini, M. Bouhelal, R. Chapman, E. Caurier, S. Courtin, E. Farnea, E. Fioretto, A. Gadea, A. Goasduff, D. Jelavić Malenica, V. Kumar, S. Lunardi, N. Mărginean, D. Mengoni, T. Mijatović *et al.*, Phys. Rev. C **87**, 054322 (2013).

[33] P. Dimitriou, I. Dillmann, B. Singh, V. Piksaikin, K. Rykaczewski, J. Tain, A. Algora, K. Banerjee, I. Borzov, D. Cano-Ott, S. Chiba, M. Fallot, D. Foligno, R. Grzywacz, X. Huang, T. Marketin, F. Minato, G. Mukherjee, B. Rasco, A. Sonzogni *et al.*, Nucl. Data Sheets **173**, 144 (2021).

[34] J. A. Winger, P. F. Mantica, and R. M. Ronningen, Phys. Rev. C **73**, 044318 (2006).

[35] L. A. Riley, D. Bazin, J. Belarge, P. C. Bender, B. A. Brown, P. D. Cottle, B. Elman, A. Gade, S. D. Gregory, E. B. Haldeman, K. W. Kemper, B. R. Klybor, M. A. Liggett, S. Lipschutz, B. Longfellow, E. Lunderberg, T. Mijatovic, J. Pereira, L. M. Skiles, R. Titus *et al.*, Phys. Rev. C **100**, 044312 (2019).

[36] B. Longfellow, D. Weisshaar, A. Gade, B. A. Brown, D. Bazin, K. W. Brown, B. Elman, J. Pereira, D. Rhodes, and M. Spieker, Phys. Rev. Lett. **125**, 232501 (2020).

[37] S. Momiyama, K. Wimmer, D. Bazin, J. Belarge, P. Bender, B. Elman, A. Gade, K. W. Kemper, N. Kitamura, B. Longfellow, E. Lunderberg, M. Niikura, S. Ota, P. Schrock, J. A. Tostevin, and D. Weisshaar, Phys. Rev. C **102**, 034325 (2020).

[38] B. Longfellow, D. Weisshaar, A. Gade, B. A. Brown, D. Bazin, K. W. Brown, B. Elman, J. Pereira, D. Rhodes, and M. Spieker, Phys. Rev. C **103**, 054309 (2021).

[39] S. R. Stroberg, A. Gade, T. Baugher, D. Bazin, B. A. Brown, J. M. Cook, T. Glasmacher, G. F. Grinyer, S. McDaniel, A. Ratkiewicz, and D. Weisshaar, Phys. Rev. C **86**, 024321 (2012).

[40] Y. Suzuki and M. Kimura, Phys. Rev. C **104**, 024327 (2021).